Resonance superfluidity: Renormalization of resonance scattering theory

S. J. J. M. F. Kokkelmans,[1] J. N. Milstein,[1] M. L. Chiofalo,[2] R. Walser,[1] and M. J. Holland[1]
[1]*JILA, University of Colorado and National Institute of Standards and Technology, Boulder, Colorado 80309-0440*
[2]*INFM and Classe di Scienze, Scuola Normale Superiore, Piazza dei Cavalieri 7, I-56126, Pisa, Italy*
(Received 14 December 2001; published 14 May 2002)

We derive a theory of superfluidity for a dilute Fermi gas that is valid when scattering resonances are present. The treatment of a resonance in many-body atomic physics requires a novel mean-field approach starting from an unconventional microscopic Hamiltonian. The mean-field equations incorporate the microscopic scattering physics, and the solutions to these equations reproduce the energy-dependent scattering properties. This theory describes the high-T_c behavior of the system, and predicts a value of T_c that is a significant fraction of the Fermi temperature. It is shown that this mean-field approach does not break down for typical experimental circumstances, even at detunings close to resonance. As an example of the application of our theory, we investigate the feasibility for achieving superfluidity in an ultracold gas of fermionic ^{6}Li.

DOI: 10.1103/PhysRevA.65.053617 PACS number(s): 03.75.Fi, 67.60.−g, 74.20.−z

I. INTRODUCTION

The remarkable accomplishment of reaching the regime of quantum degeneracy [1] in a variety of ultracold atomic gases enabled the examination of superfluid phenomena in a diverse range of novel quantum systems. Already many elementary aspects of superfluid phenomena have been observed in bosonic systems including vortices [2]. The challenge of achieving superfluidity in a Fermi gas remains, however, although it appears possible that this situation may change in the near future. A number of candidate systems for realizing superfluidity in a fermionic gas appear very promising and it is currently the goal of several experimental efforts to get into the required regime to observe the superfluid phase transition. So far both fermionic potassium [3] and lithium [4,5] have been cooled to the microkelvin regime and are well below the Fermi temperature by now—a precursor step for superfluidity.

In order to make the superfluid phase transition experimentally accessible, it will likely be necessary to utilize the rich internal hyperfine structure of atomic collisions. Scattering resonances, in particular, may prove to be extremely important since they potentially allow a significant enhancement of the strength of the atomic interactions. It is anticipated that by utilizing such a scattering resonance one may dramatically increase the critical temperature at which the system becomes unstable towards the formation of Cooper pairs, thus bringing the critical temperature into the experimentally accessible regime.

In spite of its promise, this situation poses a number of fundamental theoretical problems that must be addressed in order to provide an adequate minimal description of the critical behavior. The scope of the complexities that arise in treating a scattering resonance can be seen by examining the convergence of the quantum kinetic perturbation theory of the dilute gas. In this theory the small parameter is known as the gaseous parameter, defined as $\sqrt{na^3}$, where n is the particle density and a is the scattering length. Formally, when the scattering length is increased to the value at which $na^3 \approx 1$, conventional perturbation theory breaks down [6,7]. This situation is commonly associated with the theoretical treatment of strongly interacting fermionic systems where higher-order correlations must be treated explicitly.

In this paper, we show that an unconventional mean-field theory can still be appropriately exploited under the condition that the characteristic range R of the potential is such that $nR^3 \ll 1$ (while $na^3 \gtrsim 1$). The core issue is that around a resonance, the cross section becomes strongly dependent on the scattering energy. This occurs when either a bound state lies just below threshold, or when a quasibound state lies just above the edge of the collision continuum. In both cases, the scattering length—evaluated by considering the zero-energy limit of the scattering phase shift—does not characterize the full scattering physics over the complete energy range of interest, even when in practice this may cover a range of only a few microkelvin.

The paper is outlined as follows. In Sec. II, we present a systematic derivation of the renormalized potentials for an effective many-body Hamiltonian. This requires a detailed analysis of coupled-channels scattering. In Sec. III, we derive the resonance mean-field theory. In Sec. IV, we present the thermodynamic solutions allowing for resonance superfluidity. We apply our theory to the specific case of ^{6}Li and determine the critical temperature for the superfluid phase transition. In Sec. V, we consider the validity of the mean-field approach in the case of resonance coupling, and establish the equivalence with previous diagrammatic calculations of the crossover regime between fermionic and bosonic superconductivity.

II. TWO-BODY RESONANCE SCATTERING

The position of the last bound state in the interatomic interaction potentials generally has a crucial effect on the scattering properties. In a single-channel system, the scattering process becomes resonant when a bound state is close to threshold. In a multichannel system the incoming channel (which is always open) may be coupled during the collision to other open or closed channels corresponding to different spin configurations. When a bound state in a closed channel lies near the zero of the collision energy continuum, a Feshbach resonance [8] may occur, giving rise to scattering prop-

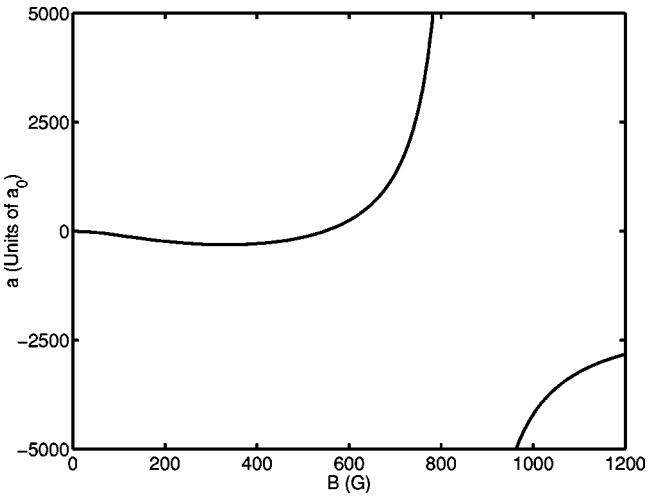

FIG. 1. Scattering length as a function of magnetic field, for the $(f,m_f)=(1/2,-1/2)$ and $(1/2,1/2)$ mixed spin channel of ^{6}Li.

erties that are tunable by an external magnetic field. The tuning dependence arises from the magnetic moment difference $\Delta\mu^{\mathrm{mag}}$ between the open and closed channels [9]. This gives rise to a characteristic dispersive behavior of the *s*-wave scattering length at fields close to resonance given by

$$a=a_{\mathrm{bg}}\left(1-\frac{\Delta B}{B-B_0}\right), \tag{1}$$

where a_{bg} is the background value that may itself depend weakly on magnetic field. The field width of the resonance is given by ΔB, and the bound state crosses threshold at a field-value B_0. The field detuning can be converted into an energy detuning $\overline{\nu}$ by the relation $\overline{\nu}=(B-B_0)\Delta\mu^{\mathrm{mag}}$. An example of such a resonance is given in Fig. 1, where a coupled-channels calculation is shown of the scattering length of ^{6}Li for collisions between atoms in the $(f,m_f)=(1/2,-1/2)$ and $(1/2,1/2)$ states [10]. The background scattering length changes slowly as a function of magnetic field due to a field-dependent mixing of a second resonance that comes from the triplet potential. This full coupled-channels calculation includes the state-of-the-art interatomic potentials [11] and the complete internal hyperfine structure [13].

The scattering length is often used in many-body theory to describe interactions in the *s*-wave regime. That the scattering length completely encapsulates the collision physics over relevant energy scales is implicitly assumed in the derivation of the conventional Bardeen-Cooper-Schrieffer (BCS) theory for degenerate gases [14,15], as well as the Gross-Pitaevskii description of Bose-Einstein condensates. However, the scattering length is only a useful concept in the energy regime where the *s*-wave scattering phase shift δ_0 depends linearly on the wave number *k*, i.e., $\delta_0=-ka$. For a Feshbach resonance system at a finite temperature there will always be a magnetic field value where this approximation breaks down and the scattering properties become strongly energy dependent. In close proximity to a resonance, the scattering process then has to be treated by means of the energy-dependent *T* matrix.

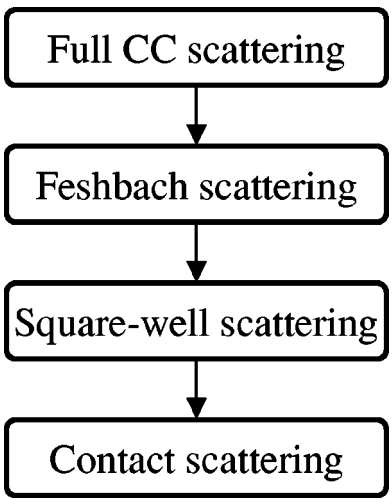

FIG. 2. Sequence of theoretical steps involved in formulating a renormalized scattering model of resonance physics for low-energy scattering. The starting point is a full coupled-channels (CC) calculation that leads us via an equivalent Feshbach theory, and an analytic coupled square-well theory, to a contact potential scattering theory that gives the renormalized equations for the resonance system.

Only the exact interatomic interaction will reproduce the full *T* matrix over all energy scales. However, since only collision energies in the ultracold regime (of order microkelvin) are relevant, a much simpler description is possible. If the scattering length does not completely characterize the low-energy scattering behavior in the presence of a resonance, what is the minimal set of parameters that will do?

As illustrated in Fig. 2, we proceed to systematically resolve this question by the following steps. We start from a numerical solution of the complete coupled-channels scattering problem for a given real physical system. In Sec. II A we demonstrate that the results of these full numerical calculations can be adequately replicated by giving an analytic description of resonance scattering provided by Feshbach's resonance theory. The point of this connection is to demonstrate that only a few parameters are necessary to account for all the collision properties. This implies that the scattering model is not unique. There are many microscopic models that could be described by the same Feshbach theory. In Sec. II B we show this explicitly by presenting a simple double-well model for which analytic solutions are accessible. Thereby we derive a limiting model in which the range of the square well potentials and coupling matrix elements are taken to zero. This leads in Sec. II C to a scattering model of contact potentials. We show that such a scattering solution is able to reproduce well the results of the intricate full numerical model we began with. The utility of this result is that, as will be apparent later, it greatly simplifies the many-body theoretic description.

A. Feshbach resonance theory

Here we briefly describe the Feshbach resonance formalism and derive the elastic *S* matrices and *T* matrices for two-

body scattering. These matrices are related to the transition probabilities for scattering from an initial channel α to a final channel β. A more detailed treatment of this formalism can be found in the literature [8].

In Feshbach resonance theory two projection operators P and Q are introduced, which project onto the subspaces $\mathcal{P}$ and $\mathcal{Q}$. These subspaces are two orthogonal components that together span the full Hilbert space of both scattering and bound wave functions. The open and closed channels are contained in $\mathcal{P}$ and $\mathcal{Q}$, respectively. The operators P and Q split the Schrödinger equation for the two-body problem into two parts:

$$(E-H_{PP})|\psi^P\rangle=H_{PQ}|\psi^Q\rangle, \tag{2}$$

$$(E-H_{QQ})|\psi^Q\rangle=H_{QP}|\psi^P\rangle, \tag{3}$$

where $H_{PP}=PHP$, $H_{PQ}=PHQ$, etc., and ψ is the total scattering wave function. The projections on the two subspaces are indicated by $P|\psi\rangle=|\psi^P\rangle$ and $Q|\psi\rangle=|\psi^Q\rangle$. The Hamiltonian $H=H_0+V$ consists of the sum of the single-particle interactions H_0 and the two-body interaction V. Equation (3) can be formally solved

$$|\psi^Q\rangle=\frac{1}{E^+-H_{QQ}}H_{QP}|\psi^P\rangle, \tag{4}$$

where $E^+=E+i\delta$ with δ approaching zero from positive values. Substituting this result into Eq. (2), the open channels equation can be written as $(E-H_{\rm eff})|\psi^P\rangle=0$, where

$$H_{\rm eff}=H_{PP}+H_{PQ}\frac{1}{E^+-H_{QQ}}H_{QP}. \tag{5}$$

The resolvant operator is now expanded in the discrete and continuum eigenstates of H_{QQ}:

$$H_{\rm eff}=H_{PP}+\sum_i\frac{H_{PQ}|\phi_i\rangle\langle\phi_i|H_{QP}}{E-\epsilon_i}+\int\frac{H_{PQ}|\phi(\epsilon)\rangle\langle\phi(\epsilon)|H_{QP}}{E^+-\epsilon}d\epsilon. \tag{6}$$

Here the ϵ_i's are the uncoupled bound-state eigenvalues. In practice, only a few bound states will significantly affect the open-channel properties. In this paper, we will consider either one or two bound states and neglect the continuum expansion in Eq. (6). Then the formal solution for $|\psi^P\rangle$ is given by

$$|\psi^P\rangle=|\psi_\alpha^{P+}\rangle+\frac{1}{E^+-H_{PP}}\sum_i\frac{H_{PQ}|\phi_i\rangle\langle\phi_i|H_{QP}|\psi^P\rangle}{E-\epsilon_i}, \tag{7}$$

where $|\psi_\alpha^{P+}\rangle$ is the eigenstate of the direct interaction H_{PP} that satisfies the outgoing wave boundary condition in channel α. By multiplying from the left with $\langle\chi_\beta|V$, where $|\chi_\beta\rangle$ is an unscattered state in the outgoing channel β, the left-hand side becomes the $\mathcal{T}$ matrix for the total scattering process. The unscattered state is related to the scattering wave function $|\psi_\beta^{P-}\rangle$ with incoming boundary conditions via

$$|\psi_\beta^{P-}\rangle=|\chi_\beta\rangle+\frac{V}{E^--H_{PP}}|\chi_\beta\rangle. \tag{8}$$

The $\mathcal{T}$ matrix giving the transition amplitude is then

$$\mathcal{T}_{\beta\alpha}=\mathcal{T}_{\beta\alpha}^P+\sum_i\frac{\langle\psi_\beta^{P-}|H_{PQ}|\phi_i\rangle\langle\phi_i|H_{QP}|\psi^P\rangle}{E-\epsilon_i}, \tag{9}$$

where $\mathcal{T}_{\beta\alpha}^P$ is the amplitude for the direct (nonresonant) process. From the $\mathcal{T}$ matrix we can easily go to the S matrix that is defined as $S_{\beta\alpha}=\langle\psi_\beta^-|\psi_\alpha^+\rangle$. Since we consider s-wave scattering only, in our case there exists a simple relation between the S matrix and $\mathcal{T}$ matrix: $S_{\beta\alpha}=1-2\pi i\mathcal{T}_{\beta\alpha}$ [16], and this allows us to rewrite Eq. (9) as

$$S_{\beta\alpha}=S_{\beta\alpha}^P-\sum_\gamma S_{\beta\gamma}^P\sum_i\frac{2\pi i\langle\psi_\gamma^+|H_{PQ}|\phi_i\rangle\langle\phi_i|H_{QP}|\psi^P\rangle}{E-\epsilon_i}. \tag{10}$$

The nonresonant factors $S_{\beta\gamma}^P$ describe the direct scattering process from an open channel γ to the outgoing channel β. Returning to Eq. (7), we can solve for the component $\langle\phi_i|H_{QP}|\psi^P\rangle$ by multiplying both sides with $\langle\phi_i|H_{QP}$.

1. Single resonance

For the case of only one resonant bound state and only one open channel, the solution of Eq. (7) gives rise to the following elastic S-matrix element (we will omit now the incoming channel label α):

$$S=S^P\left[1-\frac{2\pi i|\langle\psi^{P+}|H_{PQ}|\phi_1\rangle|^2}{E-\epsilon_1-\langle\phi_1|H_{QP}\frac{1}{E^+-H_{PP}}H_{PQ}|\phi_1\rangle}\right]. \tag{11}$$

The nonresonant S matrix is related to the background scattering length via $S^P=\exp[-2ika_{\rm bg}]$. The term in the numerator gives rise to the energy width of the resonance, $\Gamma=2\pi|\langle\psi^{P+}|H_{PQ}|\phi_1\rangle|^2$, which is proportional to the incoming wave number k and coupling constant $\overline{g_1}$ [17]. The bracket in the denominator gives rise to a shift of the bound-state energy, and to an additional width term $i\Gamma/2$. When we denote the energy shift between the collision continuum and the bound state by $\overline{\nu_1}$, and represent the kinetic energy simply by $\hbar^2k^2/m$, the S-matrix element can be rewritten as

$$S(k)=e^{-2ika_{\rm bg}}\left[1-\frac{2ik|\overline{g_1}|^2}{-\frac{4\pi\hbar^2}{m}\left(\overline{\nu_1}-\frac{\hbar^2k^2}{m}\right)+ik|\overline{g_1}|^2}\right]. \tag{12}$$

The resulting total scattering length has exactly the same dispersive line shape for the resonant scattering length as we have presented originally as Eq. (1).

2. Double resonance

Often more than one resonance may need to be considered. For example, the scattering properties for the $(1/2, -1/2)+(1/2,1/2)$ channel of ^{6}Li are dominated by a combination of two resonances: a triplet potential resonance and a Feshbach resonance. This can be clearly seen from Fig. 1, where the residual scattering length, which would arise in the absence of the Feshbach resonance coupling, would be very large and negative and vary with magnetic field. This can be compared with the value of the nonresonant background scattering length for the triplet potential for Li that is only $31a_0$, which is an accurate measure of the characteristic range of this potential. An adequate scattering model for this system therefore requires inclusion of both bound-state resonances. Since for ^{6}Li the coupling between these two bound states is small, it will be neglected in the double-resonance model presented here. The double-resonance S matrix, with again only one open channel, follows then from Eq. (10) and includes a summation over two bound states. After solving for the two components $\langle \phi_i | H_{QP} | \psi^P \rangle$ of wave function $|\psi^P\rangle$, the S matrix can be written as

$$S(k)=e^{-2ika_{\rm bg}}\left[1-\frac{2ik(|\bar{g}_1|^2\Delta_2+|\bar{g}_2|^2\Delta_1)}{ik(|\bar{g}_1|^2\Delta_2+|\bar{g}_2|^2\Delta_1)-\Delta_1\Delta_2}\right] \tag{13}$$

with $\Delta_1=(\bar{\nu}_1-\hbar^2k^2/m)4\pi\hbar^2/m$, where $\bar{\nu}_1$ and $\bar{g}_1$ are the detuning and coupling strengths for state 1. Equivalent definitions are used for state 2. Later we will show that this simple analytic Feshbach scattering model mimics the coupled-channels calculation of ^{6}Li. The parameters of this model, which are related to the positions and widths of the last bound states, can be directly found from a plot of the scattering length versus magnetic field as given, for example, by Fig. 1. The scattering length behavior should be reproduced by the analytic expression for the scattering length following from Eq. (13):

$$a=a_{bg}-\frac{m}{4\pi\hbar^2}\left(\frac{|\bar{g}_1|^2}{\bar{\nu}_1}+\frac{|\bar{g}_2|^2}{\bar{\nu}_2}\right). \tag{14}$$

The advantage of a double pole over a single-pole S-matrix parametrization is that we can account for the interplay between a potential resonance and a Feshbach resonance, which in principle can radically change the scattering properties. This interplay is not only important for the description of ^{6}Li interactions, but also for other atomic systems that have an almost resonant triplet potential, such as bosonic ^{133}Cs [18,19] and ^{85}Rb [20].

In the many-body part of this paper, Sec. III, the scattering properties are represented by a T matrix instead of an S matrix. We have shown in the above that in our case there exists a simple relation between the two, however, the definition for T in the many-body theory will be slightly different in order to give it the conventional dimensions of energy per unit density:

$$T(k)=\frac{2\pi\hbar^2 i}{mk}[S(k)-1]. \tag{15}$$

B. Coupled square-well scattering

In this subsection we describe the coupled-channels extension of a textbook single-channel square-well scattering problem. One reason that this model is interesting to study is because we can take the limit of the potential range $R\to 0$, thus giving an explicit representation of a set of coupled δ function potentials that simplifies the description in the many-body problem to follow.

The scattering equations for such a coupled system are written as

$$E\psi^P(\mathbf{r})=\left[-\frac{\hbar^2}{m}\nabla^2_{\mathbf{r}}+V^P(\mathbf{r})\right]\psi^P(\mathbf{r})+g(\mathbf{r})\psi^Q(\mathbf{r}), \tag{16}$$

$$E\psi^Q(\mathbf{r})=\left[-\frac{\hbar^2}{m}\nabla^2_{\mathbf{r}}+V^Q(\mathbf{r})+\epsilon\right]\psi^Q(\mathbf{r})+g^*(\mathbf{r})\psi^P(\mathbf{r}), \tag{17}$$

with ϵ being the energy shift of the closed channel with respect to the collision continuum and $E=\hbar^2k^2/m$ the relative kinetic energy of the two colliding particles in the center-of-mass frame. The coupled square-well model encapsulates the general properties of two-body alkali interactions. There we can divide the internuclear separation into two regions: the inner region where the exchange interaction (the difference between the singlet and triplet potentials) is much larger than the hyperfine splitting, and the outer region where the hyperfine interaction dominates. Here we make a similar distinction for the coupled square wells. In analogy to the real singlet and triplet potentials, we use for the inner region two artificial square-well potentials labeled as V_1 and V_2. We take the coupling $g(\mathbf{r})$ to be constant over the range of the square-well potentials $r<R$, and to be zero outside this range (see Fig. 3). Then the problem can be simply solved by means of basis rotations at the boundary R giving rise to simple analytic expressions. For $r>R$, we therefore consider one open channel and one closed channel, with wave numbers k_P and k_Q. In analogy with a real physical system, we can refer to the inner range channels ($r<R$) as a molecular basis, and the channel wave functions are just linear combinations of the u_1 and u_2 wave functions. At the boundary R, these wave functions have accumulated a phase $\phi_1=k_1R$ and $\phi_2=k_2R$. The coupling strength is effectively given by the basis-rotation angle θ for the scattering wave functions:

$$\begin{pmatrix} u_P(R) \\ u_Q(R) \end{pmatrix}=\begin{pmatrix} \cos\theta & -\sin\theta \\ \sin\theta & \cos\theta \end{pmatrix}\begin{pmatrix} u_1(R) \\ u_2(R) \end{pmatrix}, \tag{18}$$

allowing for an analytic solution of the scattering model. This leads to the following expression for the S matrix:

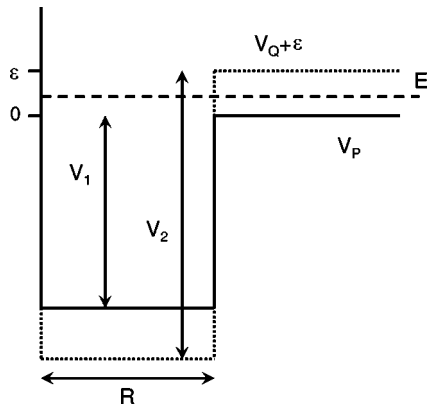

FIG. 3. Illustration of the coupled square-well system. Outer region $r>R$: the solid line corresponds to the open channel potential P, and the dotted line to the closed channel potential Q. The wave functions are given by $u_P(r)\sim\sin\langle k_P r\rangle$ and $u_Q(r)\sim\exp(-k_Q r)$, respectively. Inner region $r<R$: the solid and dotted lines correspond to the molecular potentials V_1 and V_2, respectively. The wave functions are given by $u_1(r)\sim\sin k_1 r$ and $u_2(r)\sim\sin(k_2 r)$. The dashed line corresponds to the kinetic energy E in the open channel. The wave vectors are defined as $k_P=\sqrt{mE}/\hbar$, $k_Q=\sqrt{m(\epsilon-E)}/\hbar$, $k_1=\sqrt{m(E+V_1)}/\hbar$, and $k_2=\sqrt{m(E+V_2-\epsilon)}/\hbar$. The detuning ϵ can be chosen such that a bound state of square-well potential V_2 enters the collision continuum, causing a Feshbach resonance in the open channel.

$$S=e^{-2ik_P R}[1-\{-2ik_P(k_2\cot\phi_2\cos^2\theta+k_Q+k_1\cot\phi_1\sin^2\theta)\}/\{k_P k_Q+k_1\cot\phi_1(k_P\sin^2\theta-k_Q\cos^2\theta)+ik_2\cot\phi_2(k_1\cot\phi_1+k_P\cos^2\theta+k_Q\sin^2\theta)\}]. \quad (19)$$

An extension to treat more than two coupled potentials, which would be required to model more than one resonance, is also straightforward.

The parameters of the two wells have to be chosen such that the results of a real scattering calculation are reproduced for a given physical system. In fact, all the parameters are completely determined from the field dependence of the scattering length, and all other scattering properties, such as the energy dependence of the scattering phase shift, can then be derived. First we choose a range R, typically of the order of an interatomic potential range ($100a_0$) or less. Now we have only to determine the set of parameters V_1, V_2, and θ. The potential depth V_1 is chosen such that the scattering length is equal to the background scattering length $a_{\rm bg}$, while keeping $\theta=0$. Also, V_1 should be large enough that the wave number k_1 depends weakly on the scattering energy. Then, we set θ to be nonzero, and change the detuning until a bound state crosses threshold, giving rise to a Feshbach resonance. The value of V_2 is more or less arbitrary, but we typically choose it to be larger than V_1. Finally, we change the value of θ to give the Feshbach resonance the desired width.

We will later show that the resulting scattering properties converge for $R\to 0$. In Fig. 4 the coupled square-well system is compared with the Feshbach scattering theory, for ^{40}K scattering parameters. Even despite the fact that there is a strong energy dependence of the T matrix, the two scattering representations agree very well.

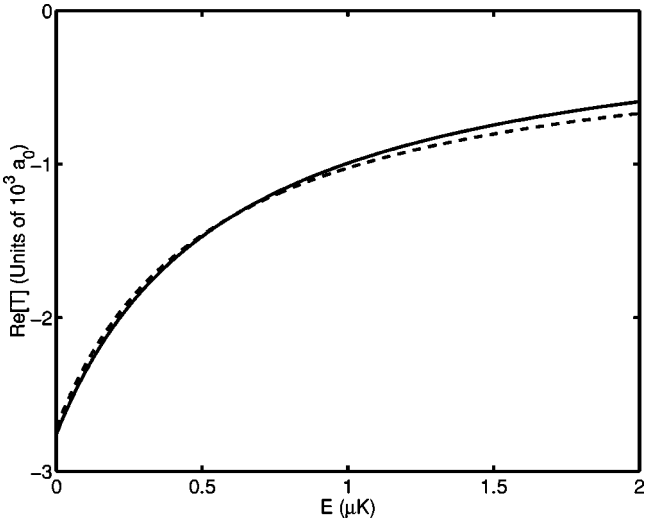

FIG. 4. Comparison of the real part of the T matrix for coupled square-well scattering (solid line) with a potential range $R=1a_0$, to Feshbach scattering (dashed line), for a detuning that yields a scattering length of about $-2750a_0$. A similar, good agreement is found for all detunings.

C. Contact potential scattering and renormalization

In this section the Lippmann-Schwinger scattering equation is solved for a resonance system with contact potentials. As in the preceding section, we make use of an open subspace that is coupled to a closed subspace. The contact potentials are defined by

$$V^P(\mathbf{r})=V^P\delta(\mathbf{r}), \quad (20)$$

$$V^Q(\mathbf{r})=V^Q\delta(\mathbf{r}),$$

$$g(\mathbf{r})=g\ \delta(\mathbf{r}), \quad (21)$$

where $\delta(\mathbf{r})$ is the three-dimensional Dirac δ function. Here $V^P(\mathbf{r})$ is the open channel potential with strength V^P. The function $V^Q(\mathbf{r})$ is a closed-channel potential with strength V^Q, and $g(\mathbf{r})$ is a coupling between the closed and open channel with strength g. The procedure of renormalization relates the physical units ($a_{\rm bg}$, $\overline{g_i}$, and $\overline{\nu_i}$) from Sec. II A to these parameters of the contact potential scattering model for a given momentum cutoff; a relationship for which we will now obtain explicit expressions. The first step is to solve again the scattering Eqs. (16) and (17) for these contact potentials. As we have seen in Sec. II A, we can formally solve the bound-state equations, and make use of Eq. (6) to expand the Green's function in bound-state solutions. In this case it can be written as

$$\psi^Q(\mathbf{r})=\sum_i \frac{\phi_i^Q(\mathbf{r})\int d^3r'\,\phi_i^{Q*}(\mathbf{r}')g^*(\mathbf{r}')\psi^P(\mathbf{r}')}{E-\epsilon_i}, \quad (22)$$

with $\phi_i^Q(\mathbf{r})$ a bound-state solution and ϵ_i its eigenenergy. We now define an amplitude for the system to be in this bound state that will later be useful in the mean-field equations: $\phi_i = \langle \phi_i^Q | \psi^Q \rangle$, and together with the open channel equation and the definition $g_i(\mathbf{r}) = g(\mathbf{r})\phi_i^Q(\mathbf{r})$, we get a new set of scattering equations,

$$\frac{\hbar^2 k^2}{m}\psi^P(\mathbf{r}) = \left[-\frac{\hbar^2}{m}\nabla_{\mathbf{r}}^2 + V^P(\mathbf{r}) \right]\psi^P(\mathbf{r}) + \sum_i g_i(\mathbf{r})\phi_i , \tag{23}$$

$$\frac{\hbar^2 k^2}{m}\phi_i = \nu_i \phi_i + \int d^3r' g_i^*(\mathbf{r}')\psi^P(\mathbf{r}'). \tag{24}$$

The energy difference between the bound-state energy and the threshold of the collision continuum is given by ν_i. The open channel solution for Eq. (23) can be formulated as

$$\begin{aligned}\psi^P(\mathbf{r}) &= \chi(\mathbf{r}) - \frac{m}{4\pi\hbar^2}\int d^3r' \frac{e^{ik|\mathbf{r}-\mathbf{r}'|}}{|\mathbf{r}-\mathbf{r}'|}\left[V^P(\mathbf{r}')\psi^P(\mathbf{r}') + \sum_i g_i(\mathbf{r}')\phi_i \right] \\ &= \chi(\mathbf{r}) + f(\theta)\frac{e^{ikr}}{r}, \quad \text{as } r\to\infty. \end{aligned} \tag{25}$$

Here $\chi(\mathbf{r})$ is the unscattered wave function, and in the other term we recognize the scattered part that is usually formulated in terms of the scattering amplitude $f(\theta)$. The momentum representation of this last line is [7]

$$\psi^P(\mathbf{p}) = (2\pi)^3\delta(\mathbf{k}-\mathbf{p}) - \frac{4\pi f(k,p)}{k^2 - p^2 + i\delta}. \tag{26}$$

Combining Eq. (26) with our expression for the scattering amplitude we find

$$-\frac{4\pi\hbar^2}{m}f(k,k') = V^P + \frac{1}{(2\pi)^3}V^P\int d^3p \frac{-\frac{4\pi\hbar^2}{m}f(k,p)}{\frac{\hbar^2k^2}{m} - \frac{\hbar^2p^2}{m} + i\delta} + \sum_i g_i\phi_i . \tag{27}$$

The typical temperature range of a system we are interested in will only allow for elastic *s*-wave scattering, therefore the scattering amplitude has no angular dependence, and incoming and outgoing wave numbers are the same, i.e., $k=k'$. The scattering amplitude can then be simply linked to the T matrix via the relation $T(k) = -(4\pi\hbar^2/m)f(k)$. The integral has a principal-value part, and the integration ranges from zero to a momentum cutoff K. Equation (27) then has as solution,

$$T(k) = V^P - \frac{V^P m}{2\pi^2\hbar^2}T(k)\left[K - \operatorname{arctanh}\frac{k}{K} + \frac{i\pi}{2}k \right] + \sum_i g_i\phi_i . \tag{28}$$

This is a variant of the Lippmann-Schwinger equation. The closed-channel scattering solutions are now used to eliminate the amplitude functions ϕ_i. In Fourier space, Eq. (24) has the form

$$\frac{\hbar^2k^2}{m}\phi_i = \nu_i\phi_i + g_i^*\frac{1}{(2\pi)^3}\int \psi^P(\mathbf{p})d^3p. \tag{29}$$

After substitution of Eq. (26) the expression for ϕ_i is linked to the T matrix:

$$\phi_i = \frac{g_i^*\left(1 - \frac{m}{2\pi^2\hbar^2}T(k)\left[K - \operatorname{arctanh}\frac{k}{K} + \frac{i\pi}{2}k \right] \right)}{\frac{\hbar^2k^2}{m} - \nu_i}. \tag{30}$$

Eliminating ϕ_i from Eq. (28) gives a complete expression for the Lippmann-Schwinger equation

$$T(k) = V^P - \frac{V^P m}{2\pi^2\hbar^2}T(k)\left[K - \operatorname{arctanh}\frac{k}{K} + \frac{i\pi}{2}k \right] + \sum_i \frac{|g_i|^2\left(1 - \frac{1}{2\pi^2}\frac{m}{\hbar^2}T(k)\left[K - \operatorname{arctanh}\frac{k}{K} + \frac{i\pi}{2}k \right] \right)}{\frac{\hbar^2k^2}{m} - \nu_i}. \tag{31}$$

Similar to the Feshbach and coupled square-well problems, the $k\to 0$ behavior of $T(k)$ should reproduce the scattering length, and, the result should not depend on the arbitrary momentum cutoff K. For an analytic expression of the scattering length, we conveniently use the Feshbach representation. A comparison between the latter and the expression for the scattering length a that results from solving Eq. (31), tells us how to relate the coupling constants for contact scattering to the Feshbach coupling constants. By making use of the definitions $\Gamma = (1-\alpha U)^{-1}$, $\alpha = mK/(2\pi^2\hbar^2)$, and $U = 4\pi\hbar^2 a_{\mathrm{bg}}/m$, we find the very concise relations

$$V^P = \Gamma U, \tag{32}$$

which is valid also in the case where no resonance is present, and in addition,

$$g_1 = \Gamma\overline{g_1}, \tag{33}$$

$$\nu_1 = \overline{\nu_1} + \alpha g_1\overline{g_1} \tag{34}$$

for the open-channel potential and the first resonance. For the second resonance, if present, we find

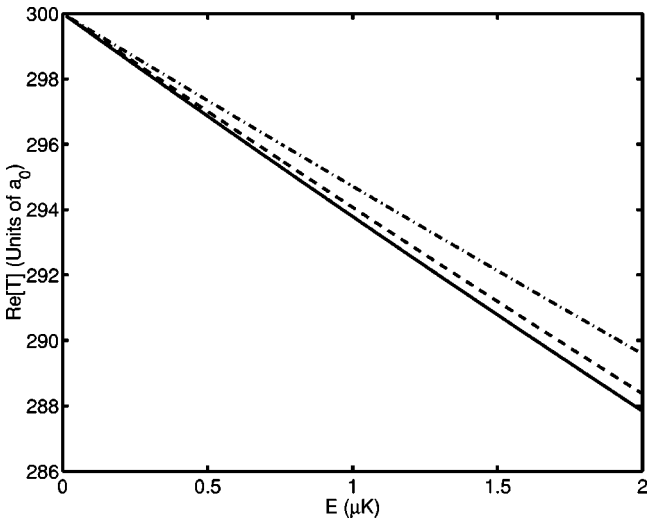

FIG. 5. Comparison of the real part of the T matrix for coupled square-well scattering for three different values of the potential range: $R=100a_0$ (dash-dotted line), $R=30a_0$ (dashed line), and $R=1a_0$ (solid line). The interaction parameters for ^{40}K have been used here, and the magnetic field is chosen such that a scattering length of $a=300a_0$ is obtained. Also plotted is the T matrix for contact scattering, which clearly agrees very well as it coincides with the solid line of the double-well scattering.

$$g_2=\frac{\overline{g}_2}{\alpha\overline{g}_1^2/\overline{\nu}_1+\Gamma^{-1}}, \tag{35}$$

$$\nu_2=\overline{\nu}_2+\alpha g_2\overline{g}_2. \tag{36}$$

Obviously, our approach can be systematically extended further, order by order, to give an arbitrarily accurate representation of the microscopic scattering physics.

These expressions we refer to as the renormalizing equations of the resonance theory since they remove the ultraviolet divergence that would otherwise appear in the field equations. Any many-body theory based on contact scattering around a Feshbach resonance will need to apply these expressions in order to renormalize the theory. These equations (32)–(36) therefore represent one of the major results of this paper.

In Fig. 5 the T matrix as a function of energy is shown for contact scattering, in comparison with the square-well scattering for different values of the potential range. The contact-scattering model is demonstrated to be the limiting case of the coupled square-well system when $R\to 0$.

D. Discussion of different models

In Sec. II C it has been shown that the resonance contact scattering representation is the limiting case of the coupled square-well system, when the range of the potentials is taken to zero. Also, in Sec. II B it has been shown that the double-well system is in good agreement with the Feshbach scattering theory. Now we will show how well these scattering representations agree with the full numerical coupled-channels calculation [10]. In Fig. 6 we show the real and

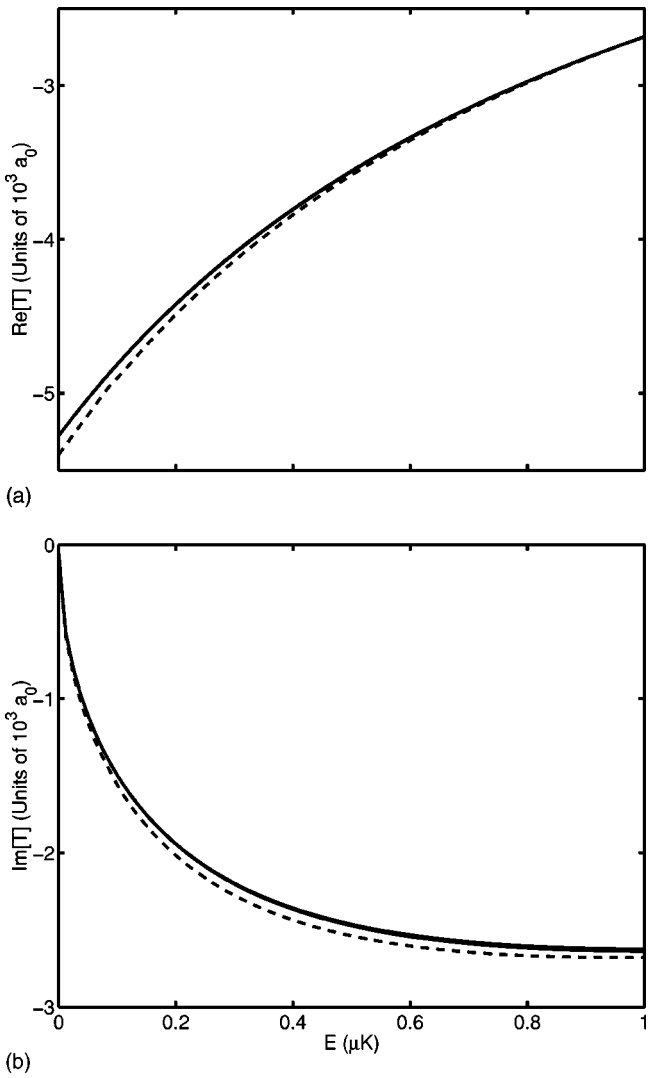

FIG. 6. (a) Real part of the T matrix as a function of collision energy, for the Feshbach model and the cutoff model (overlapping solid lines), and for a coupled-channels calculation (dashed line). The atomic species considered is ^{6}Li, for atoms colliding in the $(1/2,-1/2)+(1/2,1/2)$ channel. (b) Same as (a) for the imaginary part.

imaginary parts of the T matrix applied to the case of ^{6}Li, and compare the cutoff and Feshbach scattering representations to a full coupled-channels calculation. The agreement is surprisingly good, and holds basically for all magnetic fields (i.e., similar agreement is found at all detunings).

In this section we have discovered a remarkable fact that even a complex system including internal structure and resonances can be simply described with contact potentials and a few coupling parameters. This was known for off resonance scattering where only a single parameter (the scattering length) is required to encapsulate the collision physics at a very low temperature. However, to our knowledge this has not been pointed out before for the resonance system, where an analogous parameter set is required to describe a system where the scattering length may even pass through infinity. We have shown in a very concise set of formulas on how to derive the resonance parameters associated with contact po-

tentials. This result is important for the incorporation of the two-body scattering in a many-body system, as we will show later in this paper.

Other papers have also proposed a simple scattering model to reproduce coupled-channels calculations [21,22]. In these papers real potentials are used, and they give a fair agreement. Here, however, we use models that need input from a coupled-channels calculation to give information about the positions of the bound states and the coupling to the closed channels. All this information can be extracted from a plot of the scattering length as a function of magnetic field.

III. MANY-BODY RESONANCE SCATTERING

We will now proceed to a many-body description of resonance superfluidity and connect it to our theory of the two-body scattering problem described earlier. This section explains in detail the similar approach in our papers devoted to resonance superfluidity in potassium [23,24]. The general methods of nonequilibrium dynamics has been described in Ref. [25] and we have applied them in the context of condensed bosonic fields [26,27].

In the language of second quantization, we describe the many-body system with fermionic fields $\hat{\psi}_\sigma(\boldsymbol{x})$ that remove a single fermionic particle from position $\boldsymbol{x}$ in internal electronic state σ, and molecular bosonic fields $\hat{\phi}_i(\boldsymbol{x})$ that annihilate a composite-bound two-particle excitation from space point $\boldsymbol{x}$ in internal configuration i. These field operators and their adjoints satisfy the usual fermionic anticommutation rules

$$\{\hat{\psi}_{\sigma_1}(\boldsymbol{x}_1),\hat{\psi}^\dagger_{\sigma_2}(\boldsymbol{x}_2)\}=\delta(\boldsymbol{x}_1-\boldsymbol{x}_2)\;\delta_{\sigma_1\sigma_2}\equiv\delta_{12},$$

$$\{\hat{\psi}_{\sigma_1}(\boldsymbol{x}_1),\hat{\psi}_{\sigma_2}(\boldsymbol{x}_2)\}=0, \tag{37}$$

and bosonic commutation rules

$$[\hat{\phi}_{i_1}(\boldsymbol{x}_1),\hat{\phi}^\dagger_{i_2}(\boldsymbol{x}_2)]=\delta(\boldsymbol{x}_1-\boldsymbol{x}_2)\;\delta_{i_1i_2}\equiv\delta_{12},$$

$$[\hat{\phi}_{i_1}(\boldsymbol{x}_1),\hat{\phi}_{i_2}(\boldsymbol{x}_2)]=0, \tag{38}$$

respectively. Here and in the following discussion, we will also try to simplify the notational complexity by adopting the notation convention of many-particle physics. This means, we will identify the complete set of quantum numbers uniquely by its subscript index, i.e., $\{\boldsymbol{x}_1,\sigma_1\}\equiv 1$. If only the position coordinate is involved, we will use boldface $\boldsymbol{x}_2\equiv\mathbf{2}$. In the double-resonance case of lithium, we have to distinguish only two internal atomic configurations for the free fermionic single-particle states $\sigma=\{\uparrow,\downarrow\}$ and we need at most two indices $i=\{1,2\}$ to differentiate between the bosonic molecular resonances.

The dynamics of the multicomponent gas is governed by a total system Hamiltonian $\hat{H}=\hat{H}_0+\hat{H}_1$, which consists of the free-evolution Hamiltonian $\hat{H}_0$ and the interactions $\hat{H}_1$ between atoms and molecules. We assume that the free dynamics of the atoms and molecules is determined by their kinetic and potential energies in the presence of external traps, which is measured relative to the energy μ of a corotating reference system. Thus, we define

$$H_\sigma(\boldsymbol{x})=-\frac{\hbar^2}{2m}\nabla^2+V_\sigma(\boldsymbol{x})-\mu, \tag{39}$$

$$H^m_i(\boldsymbol{x})=-\frac{\hbar^2}{2M}\nabla^2+V^m_i(\boldsymbol{x})+\nu_i-\mu_m. \tag{40}$$

Here, m denotes the atomic mass as used previously, $M=2m$ is the molecular mass, $\mu_m=2\mu$ is the energy offset of the molecules with respect to the reference system, $V_\sigma(\boldsymbol{x})$ are external spin-dependent atomic trapping potentials, and $V^m_i(\boldsymbol{x})$ are the external molecular trapping potentials. The molecular single-particle energy has an additional energy term ν_i that accounts for the detuning of the molecular state i relative to the threshold of the collision continuum.

The binary interaction potential $V^P(\boldsymbol{x}_1-\boldsymbol{x}_2)$ accounts for the nonresonant interaction of spin-up and spin-down fermions, and coupling potentials $g_i(\boldsymbol{x}_1-\boldsymbol{x}_2)$ convert free fermionic particles into bound bosonic molecular excitations. Thus, we find for the total system Hamiltonian of the atomic and molecular fields,

$$\hat{H}=\hat{H}_0+\hat{H}_1, \tag{41}$$

where the free $\hat{H}_0$ and interaction contributions $\hat{H}_1$ are defined as

$$\hat{H}_0=\int d\mathbf{1}\sum_\sigma\;\hat{\psi}^\dagger_\sigma(\mathbf{1})H_\sigma(\mathbf{1})\hat{\psi}_\sigma(\mathbf{1}) + \int d\mathbf{1}\sum_i\;\hat{\phi}^\dagger_i(\mathbf{1})H^m_i(\mathbf{1})\hat{\phi}_i(\mathbf{1}), \tag{42}$$

$$\hat{H}_1=\int d\mathbf{1}d\mathbf{2}\left\{\hat{\psi}^\dagger_\uparrow(\mathbf{1})\hat{\psi}^\dagger_\downarrow(\mathbf{2})V^P(\mathbf{1}-\mathbf{2})\hat{\psi}_\downarrow(\mathbf{2})\hat{\psi}_\uparrow(\mathbf{1}) + \sum_i\left[\hat{\phi}^\dagger_i\left(\frac{\mathbf{1}+\mathbf{2}}{2}\right)g^*_i(\mathbf{1}-\mathbf{2})\hat{\psi}_\downarrow(\mathbf{2})\hat{\psi}_\uparrow(\mathbf{1})+\text{H.c.}\right]\right\}. \tag{43}$$

Here, H.c. denotes the Hermitian conjugate. In the present picture, we deliberately neglect the interactions among the molecules. Several other papers have treated a Feshbach resonance in a related way [28–31].

In order to derive dynamical Hartree-Fock-Bogoliubov (HFB) equations from this Hamiltonian, we also need to define a generalized density matrix to describe the state of the fermionic system [32] and an expectation value for the bosonic molecular field. The elements of the 4×4 density matrix $\mathcal{G}$ are given by

$$\mathcal{G}_{pq}(\mathbf{12})=\langle\hat{A}^\dagger_q(\boldsymbol{x}_2)\hat{A}_p(\boldsymbol{x}_1)\rangle, \tag{44}$$

$$\hat{A}(\boldsymbol{x})=[\hat{\psi}_\uparrow(\boldsymbol{x}),\hat{\psi}_\downarrow(\boldsymbol{x}),\hat{\psi}^\dagger_\uparrow(\boldsymbol{x}),\hat{\psi}^\dagger_\downarrow(\boldsymbol{x})]^\mathsf{T}, \tag{45}$$

and symmetry-broken molecular fields are defined as

$$\phi_i(\mathbf{1}) = \langle \hat{\phi}_i(\boldsymbol{x}_1) \rangle. \tag{46}$$

As usual, we define the quantum averages of an arbitrary operator $\hat{\mathcal{O}}$ with respect to a many-body density matrix $\boldsymbol{\rho}$ by $\langle \hat{\mathcal{O}} \rangle = \mathrm{Tr}[\hat{\mathcal{O}}\boldsymbol{\rho}]$, and we calculate higher-order correlation functions by a Gaussian factorization approximation known as Wick's theorem [32]. The structure of the 4×4 density matrix,

$$\mathcal{G}(\mathbf{12}) = \begin{pmatrix} \mathcal{G}_N(\mathbf{12}) & \mathcal{G}_A(\mathbf{12}) \\ -\mathcal{G}_A(\mathbf{12})^* & \mathbb{1} \times \delta_{\mathbf{12}} - \mathcal{G}_N(\mathbf{12})^* \end{pmatrix}, \tag{47}$$

is very simple, if one recognizes that it is formed out of a 2×2 single-particle density matrix $\mathcal{G}_N$, a pair correlation matrix $\mathcal{G}_A$ and obviously the vacuum fluctuations $\delta_{\mathbf{12}}$. The single-particle submatrix is given by

$$\mathcal{G}_N(\mathbf{12}) = \begin{pmatrix} \mathcal{G}_{n\uparrow}(\mathbf{12}) & \mathcal{G}_m(\mathbf{12}) \\ \mathcal{G}_m(\mathbf{21})^* & \mathcal{G}_{n\downarrow}(\mathbf{12}) \end{pmatrix}, \tag{48}$$

where $\mathcal{G}_{n\sigma}(\mathbf{12}) = \langle \hat{\psi}^\dagger_\sigma(\boldsymbol{x}_2)\hat{\psi}_\sigma(\boldsymbol{x}_1)\rangle$ is the density of spin-up and spin-down particles and $\mathcal{G}_m(\mathbf{12}) = \langle \hat{\psi}^\dagger_\downarrow(\boldsymbol{x}_2)\hat{\psi}_\uparrow(\boldsymbol{x}_1)\rangle$ denotes a cross-level coherence, or ''magnetization'' between the states. The pair-correlation submatrix $\mathcal{G}_A$ is defined analogously as

$$\mathcal{G}_A(\mathbf{12}) = \begin{pmatrix} \mathcal{G}_{a\uparrow}(\mathbf{12}) & \mathcal{G}_p(\mathbf{12}) \\ -\mathcal{G}_p(\mathbf{21}) & \mathcal{G}_{a\downarrow}(\mathbf{12}) \end{pmatrix}, \tag{49}$$

where $\mathcal{G}_{a\sigma}(\mathbf{12}) = \langle \hat{\psi}_\sigma(\boldsymbol{x}_2)\hat{\psi}_\sigma(\boldsymbol{x}_1)\rangle$ is an anomalous pairing field within the same level and the usual cross-level pairing field of BCS theory is defined here as $\mathcal{G}_p(\mathbf{12}) = \langle \hat{\psi}_\downarrow(\boldsymbol{x}_2)\hat{\psi}_\uparrow(\boldsymbol{x}_1)\rangle$.

A. General dynamic Hartree-Fock-Bogoliubov equations of motion

From these physical assumptions about the system's Hamiltonian Eq. (41) and the postulated mean fields ϕ_i of Eq. (46) and $\mathcal{G}$ of Eq. (47), one can now derive kinetic equations for the expectation values $\langle \mathcal{O} \rangle$ for an operator $\mathcal{O}$ by a systematic application of Heisenberg's equation

$$i\hbar \frac{d}{dt}\hat{\mathcal{O}} = [\hat{\mathcal{O}}, \hat{H}], \tag{50}$$

and Wick's theorem.

The first-order kinetic equation for the Hermitian density matrix $\mathcal{G}$ has the general form of a commutator and the time-evolution is determined by a Hermitian self-energy matrix $\Sigma = \Sigma^0 + \Sigma^1$. In general, one finds

$$i\hbar \frac{d}{dt}\mathcal{G}(\mathbf{13}) = \int d\mathbf{2}[\Sigma(\mathbf{12})\,\mathcal{G}(\mathbf{23}) - \mathcal{G}(\mathbf{12})\Sigma(\mathbf{23})], \tag{51}$$

$$i\hbar \frac{d}{dt}\phi_i(\mathbf{3}) = H_i^m(\mathbf{3})\,\phi_i(\mathbf{3}) + \int d\mathbf{1}d\mathbf{2}\,\delta\left(\frac{\mathbf{1}+\mathbf{2}}{2} - \mathbf{3}\right) \times g_i^*(\mathbf{1}-\mathbf{2})\mathcal{G}_p(\mathbf{12}). \tag{52}$$

First, the free-evolution Σ^0 is obviously related to the single-particle Hamiltonians of Eq. (42). In complete analogy to the generalized density matrix, it has a simple 4×4 structure

$$\Sigma^0(\mathbf{12}) = \begin{pmatrix} \Sigma^0_{\mathcal{N}}(\mathbf{12}) & 0 \\ 0 & -\Sigma^0_{\mathcal{N}}(\mathbf{12})^* \end{pmatrix}, \tag{53}$$

which can be factorized into 2×2 submatrices as

$$\Sigma^0_{\mathcal{N}}(\mathbf{12}) = \delta_{\mathbf{12}}\begin{pmatrix} H_\uparrow(\mathbf{1}) & 0 \\ 0 & H_\downarrow(\mathbf{1}) \end{pmatrix}. \tag{54}$$

Second, one obtains from the interaction Hamiltonian of Eq. (43) the first-order self-energy Σ^1 as

$$\Sigma^1(\mathbf{12}) = \begin{pmatrix} \Sigma^1_{\mathcal{N}}(\mathbf{12}) & \Sigma^1_{\mathcal{A}}(\mathbf{12}) \\ -\Sigma^1_{\mathcal{A}}(\mathbf{12})^* & -\Sigma^1_{\mathcal{N}}(\mathbf{12})^* \end{pmatrix}. \tag{55}$$

The normal potential matrix $\Sigma^1_{\mathcal{N}}$ has the usual structure of direct contributions [i.e., local Hartree potentials proportional to $\delta_{\mathbf{12}}$] and exchange terms [i.e., nonlocal Fock potentials proportional to $V^P(\mathbf{1}-\mathbf{2})$]:

$$\Sigma^1_{\mathcal{N}}(\mathbf{12}) = \int d\mathbf{4}V^P(\mathbf{2}-\mathbf{4})\begin{pmatrix} \delta_{\mathbf{12}}\mathcal{G}_{n\downarrow}(\mathbf{44}) & -\delta_{\mathbf{14}}\mathcal{G}_m(\mathbf{12}) \\ -\delta_{\mathbf{14}}\mathcal{G}_m(\mathbf{21})^* & \delta_{\mathbf{12}}\mathcal{G}_{n\uparrow}(\mathbf{44}) \end{pmatrix}. \tag{56}$$

The zeros that appear in the diagonal of the anomalous coupling matrix

$$\Sigma^1_{\mathcal{A}}(\mathbf{12}) = \begin{pmatrix} 0 & \Delta(\mathbf{12}) \\ -\Delta(\mathbf{21}) & 0 \end{pmatrix} \tag{57}$$

reflect the fact that there is no low-energy (s-wave) interaction between same spin particles due to the Pauli exclusion principle. The off-diagonal element defines a gap function as

$$\Delta(\mathbf{12}) = V^P(\mathbf{1}-\mathbf{2})\,\mathcal{G}_p(\mathbf{12}) + \sum_i g_i(\mathbf{1}-\mathbf{2})\,\phi_i\left(\frac{\mathbf{1}+\mathbf{2}}{2}\right). \tag{58}$$

B. The homogeneous limit and the contact potential approximation

In this section, we will apply the general HFB equations of motion [Eq. (51)] to the case of a spatially homogeneous isotropic system. Furthermore, we will approximate the finite-range interaction potentials $V^P(\boldsymbol{x}_1-\boldsymbol{x}_2)$ and $g_i(\boldsymbol{x}_1-\boldsymbol{x}_2)$ by the contact approximation as introduced in Eq. (20), and assume equal populations for spin-up and spin-down atoms.

Spatial homogeneity implies that a physical system is translationally invariant. Thus, any single-particle field must be constant in space and any two-particle quantity or pair-

correlation function can depend on the coordinate difference only:

$$\phi_i(\boldsymbol{x}) = \phi_i(\mathbf{0}) \equiv \phi_i\,, \tag{59}$$

$$\mathcal{G}(\boldsymbol{x}_1, \boldsymbol{x}_2) = \mathcal{G}(\boldsymbol{x}_1 - \boldsymbol{x}_2) = \mathcal{G}(\boldsymbol{r}). \tag{60}$$

This assumption implies also that there can be no external trapping potentials present, i.e., $V_\sigma(\boldsymbol{x}) = V_i^m(\boldsymbol{x}) = 0$, as this would break the translational symmetry.

Furthermore, we want to consider a special situation where there is no population difference in spin-up and spin-down particles $\mathcal{G}_n(r=|\boldsymbol{r}|) = \mathcal{G}_{n\sigma}(\boldsymbol{r})$, there exists no cross-level coherence or ''magnetization'' $\mathcal{G}_m(r) = 0$, and the anomalous pairing field $\mathcal{G}_a(r) = 0$. It is important to note that this special scenario is consistent with the full evolution equation and, on the other hand, leads to a greatly simplified sparse density matrix,

$$\mathcal{G}(\mathbf{12}) = \begin{pmatrix} \mathcal{G}_n(r) & 0 & 0 & \mathcal{G}_p(r) \\ 0 & \mathcal{G}_n(r) & -\mathcal{G}_p(r) & 0 \\ 0 & -\mathcal{G}_p^*(r) & \delta(\boldsymbol{r}) - \mathcal{G}_n(r) & 0 \\ \mathcal{G}_p^*(r) & 0 & 0 & \delta(\boldsymbol{r}) - \mathcal{G}_n(r) \end{pmatrix}, \tag{61}$$

where $r = |\boldsymbol{r}| = |\mathbf{1} - \mathbf{2}|$. Similarly, one finds a translationally invariant self-energy $\Sigma(\mathbf{12}) = \Sigma(\mathbf{1} - \mathbf{2})$ with

$$\Sigma(\mathbf{12}) = \delta_{\mathbf{12}} \begin{pmatrix} \Sigma(\mathbf{1}) & 0 & 0 & \Delta \\ 0 & \Sigma(\mathbf{1}) & -\Delta & 0 \\ 0 & -\Delta^* & -\Sigma(\mathbf{1}) & 0 \\ \Delta^* & 0 & 0 & -\Sigma(\mathbf{1}) \end{pmatrix}, \tag{62}$$

and $\Sigma(\boldsymbol{x}) = -\hbar^2/(2m)\nabla_{\boldsymbol{x}}^2 - \mu + V^P \mathcal{G}_n(0)$ and a complex energy gap $\Delta = V^P \mathcal{G}_p(0) + \Sigma_i g_i\, \phi_i$. These assumptions lead to a significant simplification of the HFB equations.

The structure of the HFB equations can be elucidated further by separating out the bare two-particle interactions from the many-body contributions. One can achieve this by splitting the self-energy into the kinetic energy and mean-field shifts $\Sigma = \Sigma^0 + \Sigma^1$, and by separating the density matrix into the vacuum contribution $\mathcal{G}^0$ [proportional to $\delta(\boldsymbol{r})$] and the remaining mean fields $\mathcal{G} = \mathcal{G}^0 + \mathcal{G}^1$:

$$i\hbar \frac{d}{dt}\mathcal{G}^1 - [\Sigma^0, \mathcal{G}^1] - [\Sigma^1, \mathcal{G}^0] = [\Sigma^1, \mathcal{G}^1], \tag{63}$$

$$i\hbar \frac{d}{dt}\phi_i = (\nu_i - \mu_m)\, \phi_i + g_i^*\, \mathcal{G}_p(0). \tag{64}$$

In this fashion, we can now identify the physics of resonance scattering of two particles in vacuo [left-hand side of Eq. (63)] from the many-body corrections due to the presence of a medium [right-hand side of Eq. (63)].

In the limit of very low densities, we can ignore many-body effects and rediscover Eqs. (23) and (24) of Sec. II C, but given here in a time-dependent form. They describe the scattering problem that we have solved already:

$$i\hbar \frac{d}{dt}\mathcal{G}_n(\boldsymbol{r}) = 0, \tag{65}$$

$$i\hbar \frac{d}{dt}\mathcal{G}_p(\boldsymbol{r}) = \left[-\frac{\hbar^2}{m}\nabla_{\boldsymbol{r}}^2 - 2\mu + V^P(\boldsymbol{r}) \right] \mathcal{G}_p(\boldsymbol{r}) + \sum_i\, g_i(\boldsymbol{r})\, \phi_i\,, \tag{66}$$

$$i\hbar \frac{d}{dt}\phi_i = (\nu_i - \mu_m)\, \phi_i + g_i^*\, \mathcal{G}_p(0). \tag{67}$$

The scattering solution of Eqs. (66) and (67) is ''summarized'' by the energy-dependent two-body T matrix, which we have discussed in the preceeding sections. In order to incorporate the full energy dependence of the scattering physics, we propose to upgrade the direct energy shift $V^P \mathcal{G}_n(\boldsymbol{r})$ to $\langle T^{\mathrm{Re}}(k) \rangle \mathcal{G}_n(\boldsymbol{r})$, where $\langle T^{\mathrm{Re}}(k) \rangle$ represents the real part of the two-body T matrix, and $\langle \cdots \rangle$ denotes two-particle thermal averaging over a Fermi distribution. A detailed calculation of the proper upgrade procedure will be presented in a forthcoming publication.

The translationally invariant HFB Equations (63) and (64) are best analyzed in momentum-space. Thus, we will introduce the Fourier transformed field-operators $\hat{a}_{\boldsymbol{k}\sigma}$ by

$$\hat{\psi}_\sigma(\boldsymbol{x}) = \sum_{\boldsymbol{k}}\, \frac{e^{-i\boldsymbol{k}x}}{\sqrt{\Omega}} \hat{a}_{\boldsymbol{k}\sigma}\,, \tag{68}$$

where Ω is the quantization volume. If we define the Fourier components of the translationally invariant mean fields as

$$\mathcal{G}(\boldsymbol{r}) = \mathcal{G}(\boldsymbol{x}_1 - \boldsymbol{x}_2) = \sum_{\boldsymbol{k}}\, e^{-i\boldsymbol{k}(\boldsymbol{x}_1 - \boldsymbol{x}_2)}\, \mathcal{G}(\boldsymbol{k}), \tag{69}$$

we obtain the following relations between the real-space density of particles n (the same for both spins) and the real-space density of particle pairs p:

$$n = \mathcal{G}_{n\sigma}(\boldsymbol{r} = 0) = \sum_{\boldsymbol{k}}\, \mathcal{G}_{n\sigma}(\boldsymbol{k}) = \frac{1}{\Omega} \sum_{\boldsymbol{k}}\, \langle \hat{a}_{\boldsymbol{k}\sigma}^\dagger \hat{a}_{\boldsymbol{k}\sigma} \rangle, \tag{70}$$

$$p = \mathcal{G}_p(\boldsymbol{r} = 0) = \sum_{\boldsymbol{k}}\, \mathcal{G}_p(\boldsymbol{k}) = \frac{1}{\Omega} \sum_{\boldsymbol{k}}\, \langle \hat{a}_{-\boldsymbol{k}\downarrow} \hat{a}_{\boldsymbol{k}\uparrow} \rangle. \tag{71}$$

The Fourier-transformed HFB equations are now local in momentum space,

$$i\hbar \frac{d}{dt}\mathcal{G}(\boldsymbol{k}) = [\Sigma(\boldsymbol{k}), \mathcal{G}(\boldsymbol{k})], \tag{72}$$

$$i\hbar \frac{d}{dt}\phi_i = (\nu_i - \mu_m)\, \phi_i + g_i^*\, p, \tag{73}$$

and the self-energy is given by

$$\Sigma(\boldsymbol{k})=\begin{pmatrix} \Sigma_k & 0 & 0 & \Delta \\ 0 & \Sigma_k & -\Delta & 0 \\ 0 & -\Delta^* & -\Sigma_k & 0 \\ \Delta^* & 0 & 0 & -\Sigma_k \end{pmatrix}. \tag{74}$$

Here, the upgraded single-particle excitation energy is now $\Sigma_k=\epsilon_k-\mu+\langle T_k^{\mathrm{Re}}\rangle n$, $\epsilon_k=\hbar^2k^2/2m$ denotes the kinetic energy and the gap energy is still defined as $\Delta=V^P p+\Sigma_i g_i\phi_i$.

IV. THERMODYNAMICS

In this paper we focus on the properties of thermodynamic equilibrium. Thermodynamic equilibrium can be reached by demanding that the grand potential $\Phi_G=-k_bT\ln\Xi$ at a fixed temperature has a minimal value. In this definition k_b is Boltzmann's constant, and Ξ the partition function $\Xi=\mathrm{Tr}[\exp(-\hat{H}_{\mathrm{diag}}/k_bT)]$. The exponent containing the diagonalized Hamiltonian reads

$$\hat{H}_{\mathrm{diag}}=\sum_i (\nu_i-\mu_m)|\phi_i|^2 + \sum_{\boldsymbol{k}} [\Sigma_k+E_k(\hat{\alpha}^\dagger_{\boldsymbol{k}\uparrow}\hat{\alpha}_{\boldsymbol{k}\uparrow}+\hat{\alpha}^\dagger_{\boldsymbol{k}\downarrow}\hat{\alpha}_{\boldsymbol{k}\downarrow}-1)], \tag{75}$$

which is a quadratic approximation to the original Hamiltonian. The energy spectrum E_k results from a local diagonalization by the Bogoliubov transformation of the self-energy matrix $\Sigma_{\boldsymbol{k}}$ at each $\boldsymbol{k}$, where the obtained quasiparticle spectrum is $E_k=\sqrt{\Sigma_k^2+\Delta^2}$. Note that the first summation term in $\hat{H}_{\mathrm{diag}}$ results from a contribution from $\mathcal{Q}$ space, and the second summation term from $\mathcal{P}$ space of Sec. II A. The rotation to Bogoliubov quasiparticles is given by the general canonical transformation

$$\begin{pmatrix} \hat{\alpha}_{\boldsymbol{k}\uparrow} \\ \hat{\alpha}^\dagger_{-\boldsymbol{k}\downarrow} \end{pmatrix}=\begin{pmatrix} \cos\theta & -e^{i\gamma}\sin\theta \\ e^{i\gamma}\sin\theta & \cos\theta \end{pmatrix}\begin{pmatrix} \hat{a}_{\boldsymbol{k}\uparrow} \\ \hat{a}^\dagger_{-\boldsymbol{k}\downarrow} \end{pmatrix}, \tag{76}$$

where $\tan 2\theta_k=|\Delta|/\Sigma_k$ is the Bogoliubov transformation angle. The quasiparticle annihilation and creation operators are indicated by $\hat{\alpha}_{\boldsymbol{k}}$ and $\hat{\alpha}^\dagger_{\boldsymbol{k}}$. In Fig. 7 we show a typical quasiparticle energy spectrum for ^{6}Li versus the single-particle kinetic energy, at a magnetic field of $B=900$ G and a temperature of $T=0.01T_F$. The figure demonstrates how well the renormalizing equations (32)–(36) work in obtaining a cutoff-independent energy spectrum. This is important because it implies that all the thermodynamics that follow will also be *cutoff* independent.

For the stationary solution the grand potential, or equivalently, the free energy, has indeed a minimum. This follows easily from setting the partial derivative of the grand potential with respect to ϕ_i to zero: $\partial\Phi_G/\partial\phi_i=0$. This gives the solution

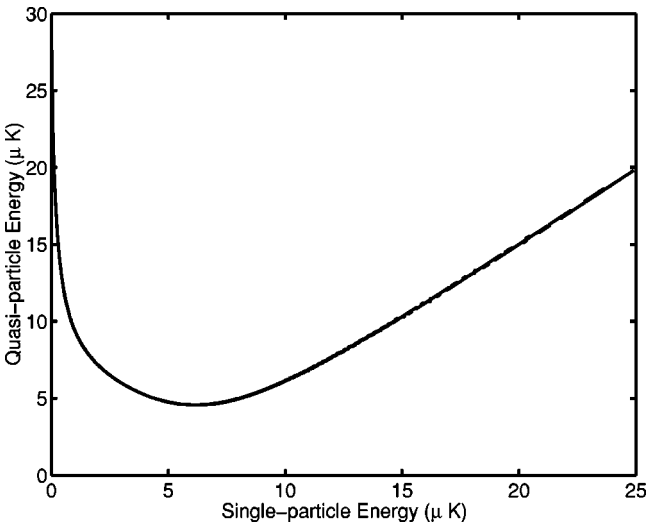

FIG. 7. Two overlapping quasiparticle energy spectra as a function of single-particle kinetic energy $E=\hbar^2k^2/(2m)$. The total density of the gas is $n=10^{14}$ cm^{-3}, the magnetic field is $B=900$ G, and the temperature is $T=0.01T_F$. The energy spectrum is calculated for two different values of the cutoff; i.e., $K=32k_F$ and $K=64k_F$. The fact that the two lines are overlapping to the extent that the difference is difficult to see shows the renormalization in practice, demonstrating the validity of Eqs. (32)–(36).

$$\phi_i=-\frac{\overline{g}_i p}{\overline{\nu}_i-\mu_m}, \tag{77}$$

which is also the stationary solution of Eq. (67). This equality is very useful because we can effectively eliminate the molecular field from the equations. The quasiparticle states are now populated according to the Fermi-Dirac distribution $n_k=[\exp(E_k/k_bT)+1]^{-1}$. The mean fields are then determined by integrating the equilibrium single-particle density matrix elements given by

$$n=\frac{1}{(2\pi)^2}\int_0^K dk\,[(2n_k-1)\cos 2\theta_k+1], \tag{78}$$

$$p=\frac{1}{(2\pi)^2}\int_0^K dk\,(2n_k-1)\sin 2\theta_k. \tag{79}$$

Since θ_k depends on n and p, these equations require self-consistent solutions that are found from a numerical iterative method.

In Fig. 8 we show a plot of the chemical potential as a function of temperature, for the case of ^{6}Li in a homogeneous gas, at a magnetic field of $B=900$ G. Figure 9 shows the ratio of the critical temperature T_c to the Fermi temperature T_F as a function of detuning. It clearly shows that there is a limiting value of T_c of about $0.5T_F$, similar to the value that has been predicted for ^{40}K in Ref. [23]. The BCS result for the critical temperature, given by the formula

$$\frac{T_c}{T_F}\sim\exp\left[-\frac{\pi}{2|a|k_F}\right], \tag{80}$$

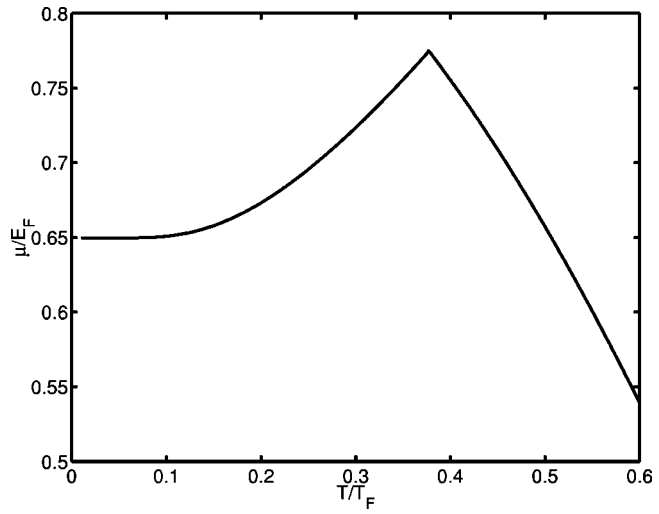

FIG. 8. Chemical potential as a function of temperature, for a magnetic field of $B=900$ G for ^{6}Li.

has been plotted in the same graph for comparison. The BCS line gives a curve for T_c higher than the resonance theory, since it does not contain the energy dependence of the T matrix. The absolute value of the scattering length in this magnetic field range is always larger than $2000a_0$, which implies that $k_F|a|>1$—a clear indication that the BCS theory breaks down in this regime.

So far, our calculation has been done for a homogeneous gas. We will also present results for a trapped lithium gas in a harmonic oscillator potential $V(\boldsymbol{r})$ with a total number of $N=5\times10^5$ atoms, similar to what we presented for ^{40}K in Ref. [24]. We treat the inhomogeneity by making use of the semiclassical local-density approximation, which involves mainly the replacement of the chemical potential by a spatially dependent version $\mu(\boldsymbol{r})=\mu-V(\boldsymbol{r})$. The thermodynamic equations for the homogeneous system are then solved at each point in space [24]. As a result, we obtain a spatially dependent density distribution. At zero temperature, for a

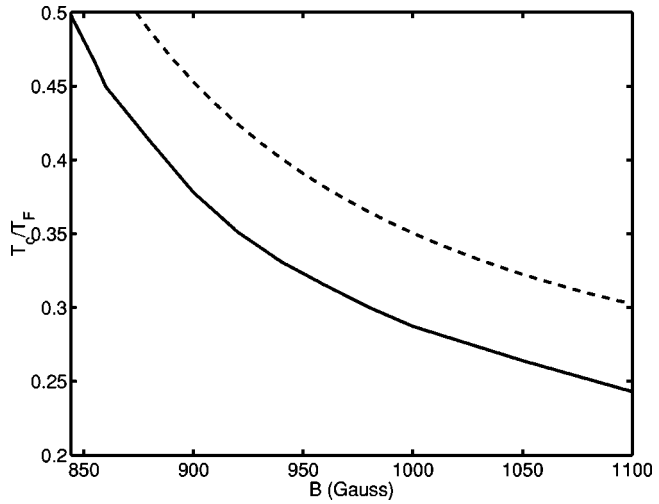

FIG. 9. Dependence of critical temperature on magnetic field for ^{6}Li, for a total density of $n=10^{14}$ cm^{-3} (solid line). The dashed line is, for comparison, the prediction of the regular BCS theory.

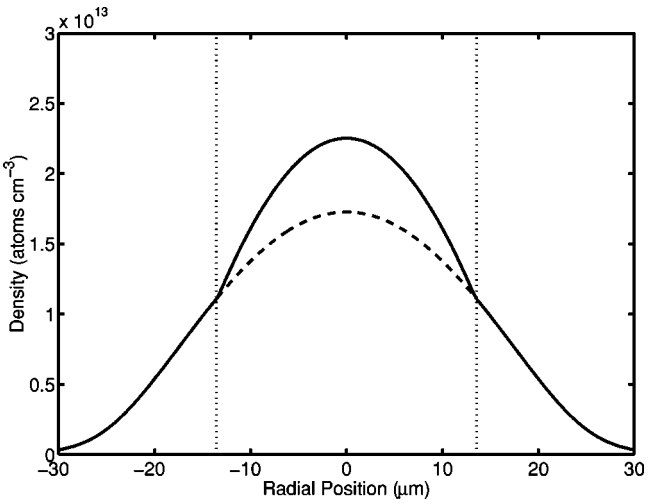

FIG. 10. Density profile for a gas of ^{6}Li atoms (solid line), evenly distributed among the two lowest hyperfine states. The temperature is $T=0.2T_F$ at a magnetic field of $B=900$ G. The trap constant is $\omega=2\pi\times500$ s^{-1}, and we have a total number $N=5\times10^5$ atoms. We compare this with a profile resulting from the same μ (but for different total number N), where artificially no superfluid is present by setting the pairing field p equal to zero (dashed line).

nonsuperfluid system, this gives the well-known Thomas-Fermi solution. For a resonance system, however, a density bulge appears in the center of the trap, which is caused by a change in compressibility when a superfluid is present. This is shown in Fig. 10, for a spherical trap with a trap constant of $\omega=2\pi\times500$ s^{-1}. This bulge is a signature of superfluidity and could experimentally be seen by fitting the density distribution in the outer wings to a nonresonant system, and thus obtaining an excess density in the middle of the trap. For a discussion of the abrupt change in the compressibility, see Ref. [24].

V. FLUCTUATIONS IN THE MEAN FIELDS AND CROSSOVER MODEL

In this section we make some comments on the connection between the resonance superfluidity theory we have presented and related mean-field approaches to discuss the crossover of superconductivity from weak to strong coupling. In the mean-field theory of BEC, most often reflected in the literature by the Gross-Pitaevskii equation or finite-temperature derivatives, a small parameter is derived to justify the application of the theory. This parameter, $\sqrt{na^3}$ [6], may be obtained from a study of higher-order corrections to the quasiparticle energy spectrum. It has been suggested that for a fermi system that exhibits superfluidity the small parameter is given by a power of k_Fa, and that the BCS theory breaks down when this parameter approaches unity. However, the small parameter in the theory of resonance superfluidity cannot be simply a function of the scattering length for detunings close to resonance. This can already be seen from the energy dependence of the T matrix, which shows that around the Fermi energy, the T matrix may have an

absolute value much smaller than at zero energy where the scattering length is defined. Moreover, even right on resonance when $\nu=0$ and the scattering length passes through infinity, the T matrix remains well behaved.

Instead of calculating the small parameter of this system, we choose a different approach based on crossover models between BCS and BEC, formulated by Nozières and Schmitt-Rink [33], and later expanded upon by Randeria [34]. In the regular BCS theory for weakly coupled systems the value of the critical temperature is given by the exponential dependence in Eq. (80), but for strongly coupled systems this model results in a logarithmically divergent prediction for T_c. The parameter $(k_F a)^{-1}$ is usually taken to describe the crossover from the weak-coupling Bose limit $[(k_F a)^{-1} \rightarrow -\infty]$ to the strong-coupling $[(k_F a)^{-1} \rightarrow +\infty]$ BEC limit. The unphysical divergence in T_c occurs because the process that dominates the transition in the weak-coupling regime is the dissociation of pairs of fermions. For a strongly coupled system, however, the fermions are so tightly bound that the wave functions of pairs of atoms begin to overlap, and the onset of coherence is signaled by excitations of the condensed state, which occurs at a temperature well below the dissociation temperature of the Cooper pairs. Thus, when moving from weak to strong coupling, the nature of the transition changes from a BCS- to a BEC-type mechanism. An explicit inclusion of the process of molecule formation, characterized by the detuning, resonance width, and resonance position, will allow us to move from one regime to the other.

The lowest-order correction that connects between BCS- and BEC-type superconductivities can be made by augmenting the density equation to account for the formation of pairs of atoms. This is done by using the thermodynamic number equation $N=-\partial\Phi_G/\partial\mu$, with Φ_G the total thermodynamic grand potential

$$\Phi_G=\Phi_G^0-k_bT\Sigma_{\mathbf{q},iq_l}\ln\Gamma(\mathbf{q},iq_l). \tag{81}$$

The term Φ_G^0 is a grand potential that does not include the quasibound molecules and results from regular BCS theory. Retaining only this term yields a theory that can only account for the free and scattered fermionic atoms that contribute to the fermion density, therefore the theory breaks down if a sizeable number of bound states are formed. In the extreme limit of strong coupling, Φ_G^0 becomes negligible and Eq. (81) just reduces to the thermodynamic potential of an ideal Bose gas. In this regime, the theory predicts the formation of a condensate of molecules below the BEC transition temperature.

The function $\Gamma(\mathbf{q},iq_l)$, which is a function of momentum $\mathbf{q}$ and thermal frequencies iq_l, is mostly negligible for a weakly coupled system and has little effect on the value of T_c in this regime. It allows for the inclusion of the lowest contributing order of quantum fluctuations [33,34] by means of a general inclusion of mechanisms for molecular pair formation. In the resonance superfluidity model, a similar term is present due to the formation of bosonic molecular bound states ϕ_i, and prevents the critical temperature from diverging. When the coupling increases, the formation of molecules adds significantly to the total density equation in both the crossover models of superconductivity and in the theory we have presented here. Moreover, the inclusion of the molecular term allows for a smooth interpolation between the BCS and BEC limits. This is clearly a substantial topic in its own right, and will be addressed further in a future publication [35].

VI. CONCLUSIONS

We have shown that it is possible to derive a mean-field theory of resonance superfluidity, which can be applied to ultracold Fermi gases such as ^{6}Li and ^{40}K. The Hamiltonian we use treats the resonant states explicitly, and automatically builds the coupled scattering equations into the many-body theory. With a study of analytical scattering we have shown that these scattering equations can completely reproduce a full coupled-channels calculation for the relevant energy regime. The energy dependence of the *s*-wave phase shifts can be described by a small set of parameters that correspond to physical properties, such as the nonresonant background value of the scattering length, and the widths and detunings of the Feshbach resonances. Close to resonance, we predict a large relative value of $0.5T_F$ for the critical temperature. The particular resonance under study for ^{6}Li occurs in the $(1/2,1/2)+(1/2,-1/2)$ collision channel, and has its peak at $B_0=844$ G, and a width of about $\Delta B\approx 185$ G [10,11]. This large width translates into a large magnetic field range where the critical temperature is within a factor of 2 from its peak value. This range is, for comparison, much larger than for ^{40}K. For ^{6}Li there are also two other Feshbach resonances, one in the $(1/2,1/2)+(3/2,-3/2)$ state, as also noted by O'Hara *et al.* [36], and another in the $(1/2,-1/2)+(3/2,-3/2)$ state. They result from coupling to the same singlet bound state, and occur at field values of about $B_0=823$ G and $B_0=705$ G, and have a similar width to the $(1/2,1/2)+(1/2,-1/2)$ resonance. The disadvantage of these resonances, however, is that the atoms in these channels suffer from dipolar losses, which are also resonantly enhanced. Three-body interactions will be largely suppressed, as asymptotic *p*-wave collisions will give very little contribution in the temperature regime considered (an *s*-wave collision is always forbidden for at least one of the pairs). From a study of crossover models between BCS and BEC we find no indication of breakdown effects of the applied mean-field theory.

ACKNOWLEDGMENTS

We thank J. Cooper, E. Cornell, D. Jin, C. Wieman, B. J. Verhaar, and B. DeMarco for very stimulating discussions. Support is acknowledged for S.J.J.M.F.K. and J.N.M. from the U.S. Department of Energy, Office of Basic Energy Sciences via the Chemical Sciences, Geosciences and Biosciences Division, and for M.L.C. from SNS, Pisa (Italy). Support is acknowledged for M.J.H. and M.L.C. from the National Science Foundation, and for R.W. from the Austrian Academy of Sciences.

[1] M.H. Anderson, J.R. Ensher, M.R. Matthews, C.E. Wieman, and E.A. Cornell, Science **269**, 198 (1995); K.B. Davis, M.-O. Mewes, M.R. Andrews, N.J. van Druten, D.S. Durfee, D.M. Kurn, and W. Ketterle, Phys. Rev. Lett. **75**, 3969 (1995); C.C. Bradley, C.A. Sackett, J.J. Tollett, and R.G. Hulet, *ibid.* **75**, 1687 (1995); **79**, 1170(E) (1997).

[2] J.E. Williams and M.J. Holland, Nature (London) **401**, 568 (1999); M.R. Matthews *et al.*, Phys. Rev. Lett. **83**, 2498 (1999); K.W. Madison, F. Chevy, W. Wohlleben, and J. Dalibard, *ibid.* **84**, 806 (2000); P.C. Haljan, I. Coddington, P. Engels, and E.A. Cornell, *ibid.* **87**, 210403 (2001); J.R. Abo-Shaeer, C. Raman, J.M. Vogels, and W. Ketterle, Science **292**, 476 (2001).

[3] B. DeMarco and D.S. Jin, Science **285**, 1703 (1999).

[4] G. Truscott, K.E. Strecker, W.I. McAlexander, G.B. Partridge, and R.G. Hulet, Science **291**, 2570 (2001).

[5] F. Schreck, L. Khaykovich, K.L. Corwin, G. Ferrari, T. Bourdel, J. Cubizolles, and C. Salomon, Phys. Rev. Lett. **87**, 080403 (2001); S. R. Granade, M. E. Gehm, K. M. O'Hara, and J. E. Thomas, *ibid.* **88**, 120405 (2002).

[6] S.T. Beliaev Zh. Eksp. Teor. Fiz. **34**, 433 (1958) [Sov. Phys. JETP **34**, 299 (1958)].

[7] A. A. Abrikosov, L. P. Gorkov, and I. E. Dzyaloshinski, *Methods of Quantum Field Theory in Statistical Physics* (Prentice-Hall, New Jersey, 1963).

[8] H. Feshbach, Ann. Phys. (N.Y.) **5**, 357 (1958); **19**, 287 (1962); H. Feshbach, *Theoretical Nuclear Physics* (Wiley, New York, 1992).

[9] E. Tiesinga, B.J. Verhaar, and H.T.C. Stoof, Phys. Rev. A **47**, 4114 (1993).

[10] S. Kokkelmans and B. J. Verhaar (private communication). The calculation is based on the analysis of the lithium interactions as described in Ref. [11]. An alternative analysis has been described in Ref. [12].

[11] F.A. van Abeelen, B.J. Verhaar, and A.J. Moerdijk, Phys. Rev. A **55**, 4377 (1997).

[12] E.R.I. Abraham *et al.*, Phys. Rev. A **55**, R3299 (1997).

[13] H.T.C. Stoof, J.M.V.A. Koelman, and B.J. Verhaar, Phys. Rev. B **38**, 4688 (1988).

[14] J. Bardeen, L.N. Cooper, and J.R. Schrieffer, Phys. Rev. **108**, 1175 (1957); J.R. Schrieffer, *Theory of Superconductivity* (Perseus Books, Reading, Massachusetts, 1999).

[15] A.G. Leggett, J. Phys. (Paris) **C7**, 19 (1980); M. Houbiers and H.T.C. Stoof, Phys. Rev. A **59**, 1556 (1999); G. Bruun *et al.*, Eur. Phys. J. D **7**, 433 (1999); H. Heiselberg, C.J. Pethick, H. Smith, and L. Viverit, Phys. Rev. Lett. **85**, 2418 (2000).

[16] J.R. Taylor, *Scattering Theory* (Wiley, New York, 1972).

[17] A.J. Moerdijk, B.J. Verhaar, and A. Axelsson, Phys. Rev. A **51**, 4852 (1995).

[18] S.J.J.M.F. Kokkelmans, B.J. Verhaar, and K. Gibble, Phys. Rev. Lett. **81**, 951 (1998).

[19] P.J. Leo, E. Tiesinga, P.S. Julienne, D.K. Walter, S. Kadlecek, and T.G. Walker, Phys. Rev. Lett. **81**, 1389 (1998).

[20] E.G.M. van Kempen, S.J.J.M.F. Kokkelmans, D.J. Heinzen, and B.J. Verhaar, Phys. Rev. Lett. **88**, 093201 (2002).

[21] M. Houbiers, H.T.C. Stoof, W.I. McAlexander, and R.G. Hulet, Phys. Rev. A **57**, R1497 (1998).

[22] J.M. Vogels, B.J. Verhaar, and R.H. Blok, Phys. Rev. A **57**, 4049 (1998).

[23] M. Holland, S.J.J.M.F. Kokkelmans, M.L. Chiofalo, and R. Walser, Phys. Rev. Lett. **87**, 120406 (2001).

[24] M.L. Chiofalo, S.J.J.M.F. Kokkelmans, J.N. Milstein, and M. Holland, Phys. Rev. Lett. **88**, 090402 (2002).

[25] A.I. Akhiezer and S.V. Peletminskii, *Methods of Statistical Physics* (Pergamon Press, Oxford, England, 1981).

[26] R. Walser, J. Williams, J. Cooper, and M. Holland, Phys. Rev. A **59**, 3878 (1999).

[27] R. Walser, J. Cooper, and M. Holland, Phys. Rev. A **63**, 013607 (2001).

[28] E. Timmermans *et al.*, Phys. Rev. Lett. **83**, 2691 (1999).

[29] F.A. van Abeelen and B.J. Verhaar, Phys. Rev. Lett. **83**, 1550 (1999).

[30] M. Holland, J. Park, and R. Walser, Phys. Rev. Lett. **86**, 1915 (2001)

[31] S.J.J.M.F. Kokkelmans, H.M.J. Vissers, and B.J. Verhaar, Phys. Rev. A **63**, 031601 (2001).

[32] J.P. Blaizot and G. Ripka, *Quantum Theory of Finite Systems* (The MIT Press, Cambridge, MA, 1986).

[33] P. Nozières and S. Schmitt-Rink, J. Low Temp. Phys. **59**, 195 (1982).

[34] See M. Randeria in *Bose-Einstein Condensation*, edited by A. Griffin, D.W. Snoke, and S. Stringari (Cambridge University Press, Cambridge, 1995).

[35] J. N. Milstein, S. J. J. M. F. Kokkelmans, and M. J. Holland, e-print cond-mat/0204334.

[36] K. M. O'Hara, M. E. Gehm, S. R. Granade, S. Bali, and J. E. Thomas, Phys. Rev. Lett. **85**, 2092 (2000).